



Applications of Spark Plasma Sintering

Takashi Goto

Institute for Materials Research, Tohoku University, Japan

2nd International school-seminar "Perspective technology of materials
consolidation with electromagnetic fields"
1st Russia-Japan SPS Workshop
Moscow, Russia, May 2022, 2013

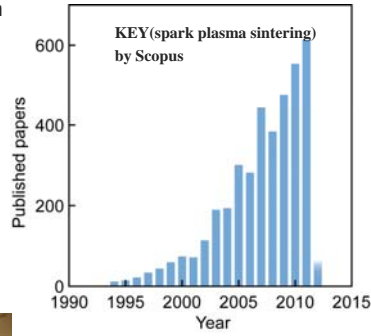
 IMR, Tohoku University

Outline

- Introduction
 - ✓ Spark Plasma Sintering (SPS)
- Transparent Lu-based Oxide Ceramics by SPS
 - ✓ Lu_2O_3 , $\text{Lu}_3\text{Al}_5\text{O}_{12}$ (LuAG), $\text{Lu}_2\text{Ti}_2\text{O}_7$, Lu_3NbO_7 , $\text{Lu}_2\text{Hf}_2\text{O}_7$
- Non-Oxide High-Temperature Ceramic Composite by SPS
 - ✓ Carbide-Boride Eutectic Composite (SiC-ZrB_2)
- Covalent Bond Ceramic Composite by SPS
 - ✓ cBN-Based Composites
- Summary

SPS Forum of Japan

- 1990 SPS Started in Japan
- 1992 First SPS in IMR
- 1996 Forum in IMR
- 2000 Forum in IMR
- 2006 New SPS in IMR
- 2009 Forum in IMR
- 2012 17th Forum in IMR



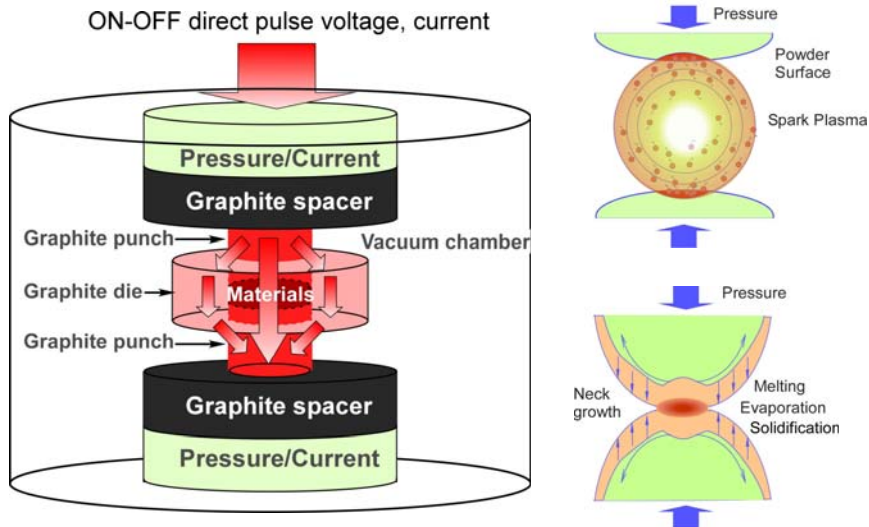
Papers of SPS



小型の低価格機開発
 放電プラズマ焼結装置 基礎研究に対応
 SPS シンデックス
 双日グループのSPS (放電プラズマ焼結) 装置(用語参照)「ドク 大学金属材料研究所の後
 シンデックス(川崎市高 津区、西嶋英一社長、0 44・820・831 ニアール写真)を開発し、コストダウンを図った。
 1)は小型卓上型のSP 装置をベースに小型化、サイズは幅1200×

2016.5.15

Spark Plasma Sintering



Transparent Materials

Single crystal



- High transparency
- Expensive, size and composition limitation, brittle

Polycrystalline

- Opaque
- Cost effective, no size-limit, wide range of composition, good mechanical property

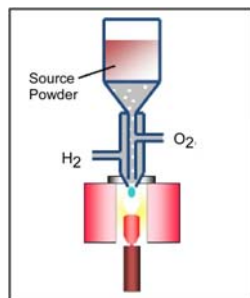


1950s: First translucent Al_2O_3 ceramics were prepared (R.L. Coble), but contained many scattering sources: pores, grain boundary phases

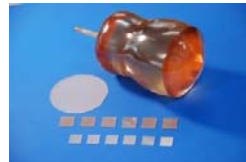
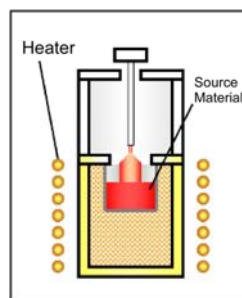
1990s: Laser oscillation was demonstrated using Nd:YAG ceramics (A. Ikesue).

- Polycrystalline ceramics with no pores, no secondary phases, less defects and atomically clean grain boundary can be transparent.
 - We can prepare transparent ceramics having high melting point, which are difficult to grow single crystals.
 - Ceramics sometimes shows excellent property than single crystals.

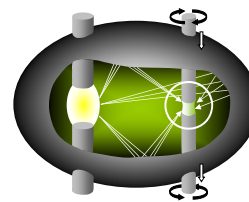
Transparent Single Crystalline Ceramics



Verneuil Method



Czochralski Method



Floating Zome Method

Spark Plasma Sintering (SPS)



Characteristics:

- Consolidation in a **short time** and at a relatively **low sintering temperature**
- Precise pressure control
- High speed cooling

Strategy

- Easy way
- Cost-effective
- Short-time
- Low-temperature

Common commercial powder source



SPS and Post-annealing



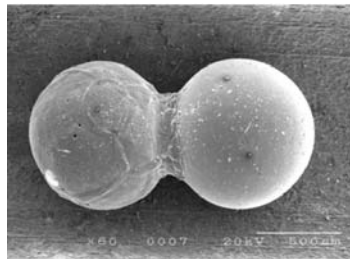
Transparent ceramics

小型の低価格機開発
 放電プラズマ焼結装置 基礎研究に対応
 SPS シンス
 テック

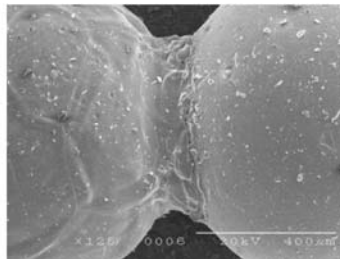
双日ケルプのSPS（放電プラズマ焼結）装置（用器参照）（トク 藤孝教授と共同開発の後シンテックス（川崎市高 津区 西崎英一社長、0 44・820・831 ニアール写真）を開発し、コストダウンを図った。）は小型卓上型のSPS た。近く販売する。東北 サブスは幅1000mm

Sintering Mechanism

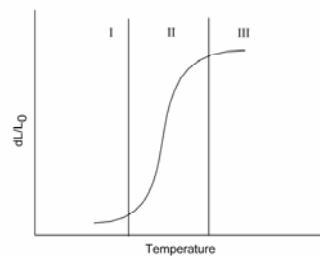
Cu



Ni

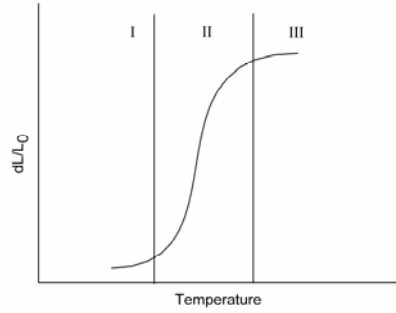


- 1st Stage (Density < 65%)
Neck growth and re-agangement of particle
- 2nd Stage (Density = 65~92%)
Continuous pore channel
Spherical to polygonal pores
- 3rd Stage (Density > 92%)
Diffusion and disappear of pores through grain-boundary



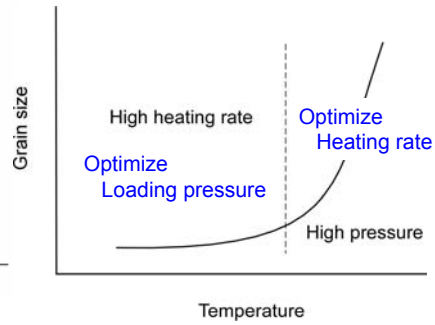
Spark Plasma Sintering (SPS)

Shrinkage curve during SPS



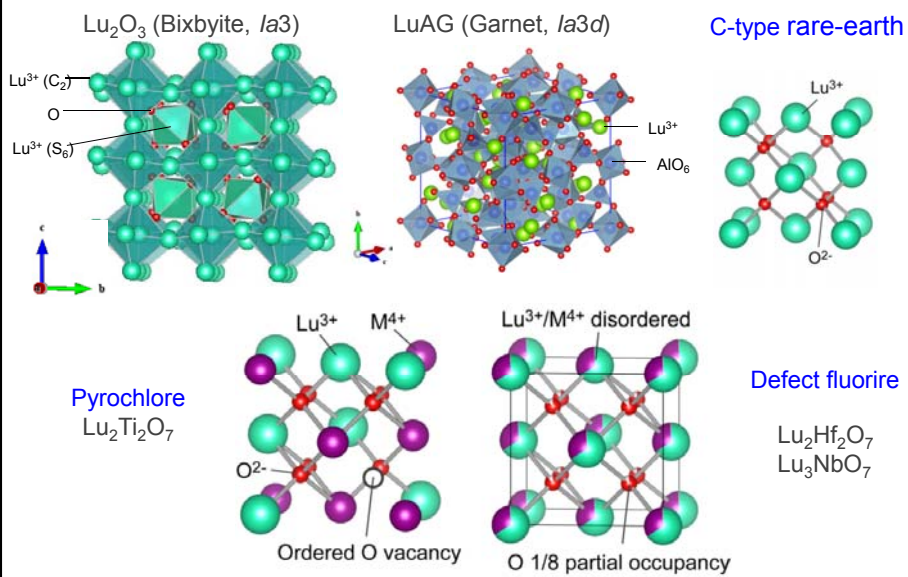
- I. Increased packing density
- II. Sintering with increased grain sliding and diffusion
- III. Removal of the pores via diffusional creep

Grain growth during SPS



- Two-step sintering profile
for no/minimal grain growth
- I & II. Pressure loading
 - III. Heating rate

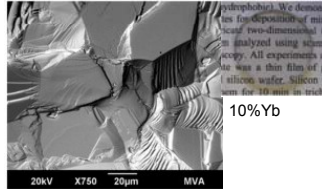
Lutetium (Lu)-based Oxides



Lutetium (Lu)-based Oxides

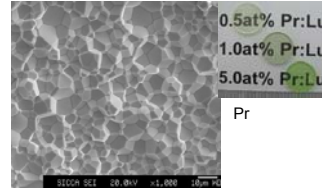
- **Practical transparent Lu-based oxide**

Lu_2O_3
(Hot pressing + Hot isostatic pressing)



J. Sanghera, et al., Opt. Mater., 33, 670-4 (2011).

$\text{Lu}_3\text{Al}_5\text{O}_{12}$ (LuAG)
(Vacuum sintering)



Y. Shi, et al., J. Appl. Phys., 109, 013522 (2011).

Main issues: **High sintering temperature** and **large grains**

There is no report on Lu_2O_3 and LuAG prepared by SPS.

- **New Lu-based oxides**

There is no report on **optical property** of Lu-based oxide single crystal and sintered body.

Introduction - Lu_2O_3

Previous study on transparent Lu_2O_3 ceramic

Sample	Synthesis method	Sintering conditions	Grain size	Transmittance at 550 nm (Thickness)	Reference
5 at% Eu: Lu_2O_3	VS	1973 K for 5 h	In nano range	Not given (translucent)	E. Zych, J. Alloy. Compd., 34, 391-4 (2002).
5 at% Eu: Lu_2O_3	NPS(H_2)	2123 K for 6 h	50–60 μm	80% (1 mm)	Q.W. Chen, J. Am. Ceram. Soc., 89, 2038-42 (2006).
3 at% Nd: Lu_2O_3	NPS(H_2)	2153 K for 8 h	~50 μm	64% (1.4 mm) 50% for Lu_2O_3	D. Zhou, J. Am. Ceram. Soc., 92, 2182-7 (2009)

VS: vacuum sintering, NPS(H_2): pressureless sintering in H_2

- **Transparent Lu_2O_3** ceramics have been prepared by conventional sintering techniques.
- The main issues are **high sintering temperature (over 1973 K)**, **long sintering time (> 5 h)** and **large grains (> 50 μm)**.

There is no report on preparation of Lu_2O_3 by SPS.

Polycrystalline Ceramic Process

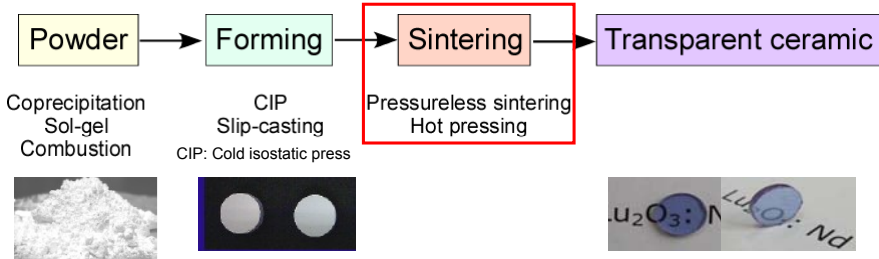


Table 1 Sintering techniques to prepare transparent ceramic

	Vacuum sintering	Pressure-less sintering in H ₂	Hot pressing	Hot isostatic pressing
Sintering Temperature	High	High	Medium	Medium
Sintering time	Long	Long	Long	Long
Grain size	Large	Large	Medium	Small

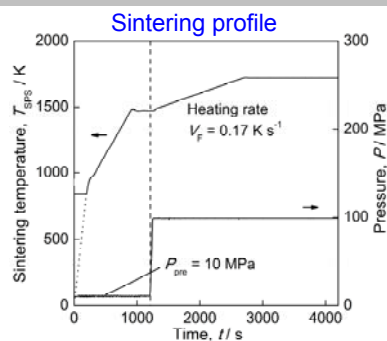
Issues:

- Home-made powder
- High sintering temperature
- Long sintering time
- Large grains

Experimental Procedure

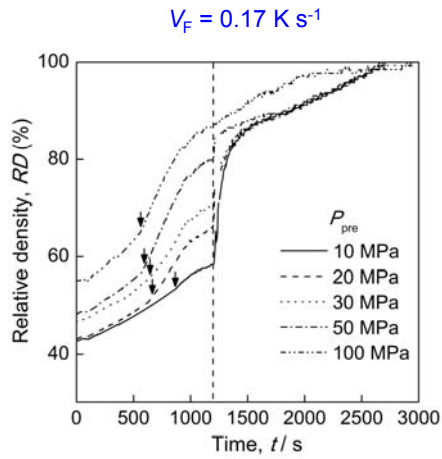


STEP I

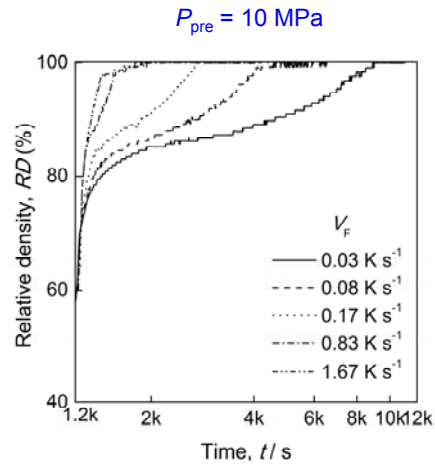


Preload pressure (P_{pre})	10-100 MPa
Final Pressure	100 MPa
Heating rate (V_F)	0.08-1.67 K s ⁻¹
Sintering temperature	1723 K
Holding time	2.7 ks
Phase	XRD
Microstructure and grain size (d):	FESEM
Relative density (RD)	Archimedes method
Transmittance (T)	UV-VIS-IR

Sintering Curves of Lu_2O_3 at Different P_{pre} and V_F



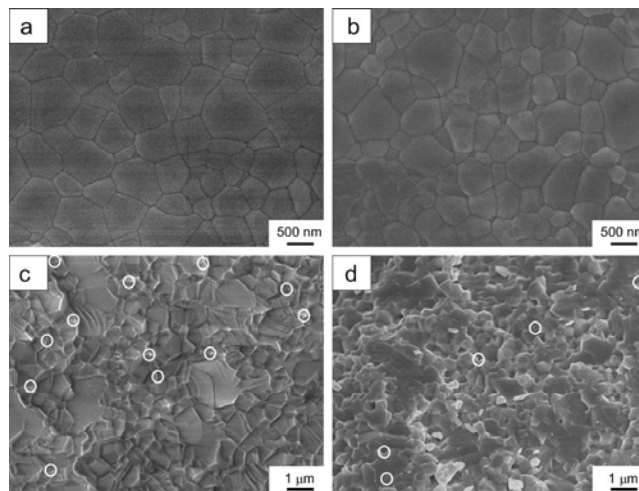
- Relative density increased significantly at the point where final pressure was applied under low P_{pre} .



- Relative density increased significantly at a high heating rate.

Journal of the European Ceramic Society, 31(2011) 1597. An, Ito, Goto

Effect of P_{pre} on Microstructure of Lu_2O_3 at $V_F = 0.17 \text{ K s}^{-1}$

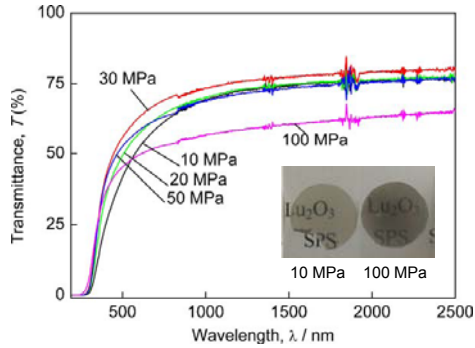
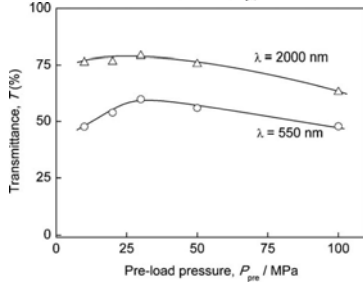
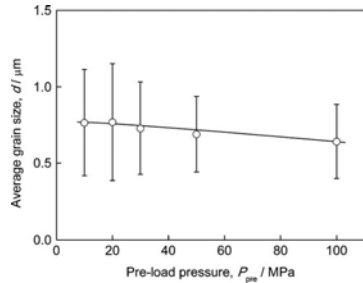


$P_{\text{pre}} = 10 \text{ MPa}$

$P_{\text{pre}} = 100 \text{ MPa}$

- Grain size decreased with increasing final pressure.

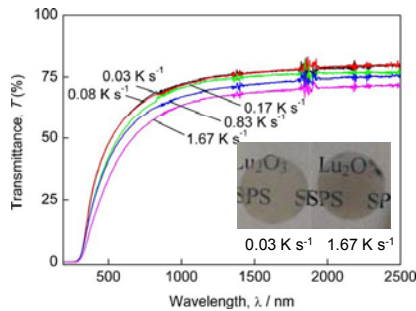
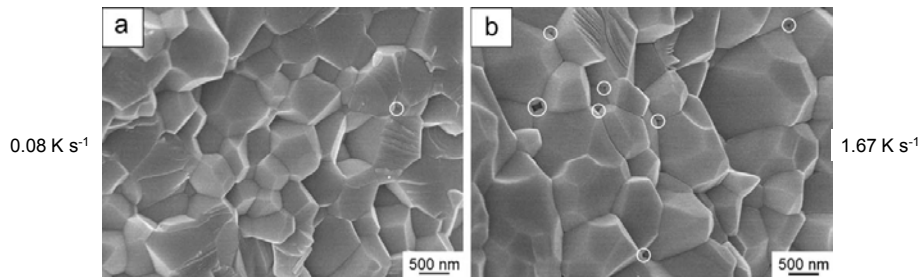
Effect of P_{pre} on Microstructure and Transmittance of Lu_2O_3



- Grain size decreased with increasing final pressure.
- Transmittance exhibited the maximum at $P_{pre}=30$ MPa

at $V_F = 0.17 \text{ K s}^{-1}$

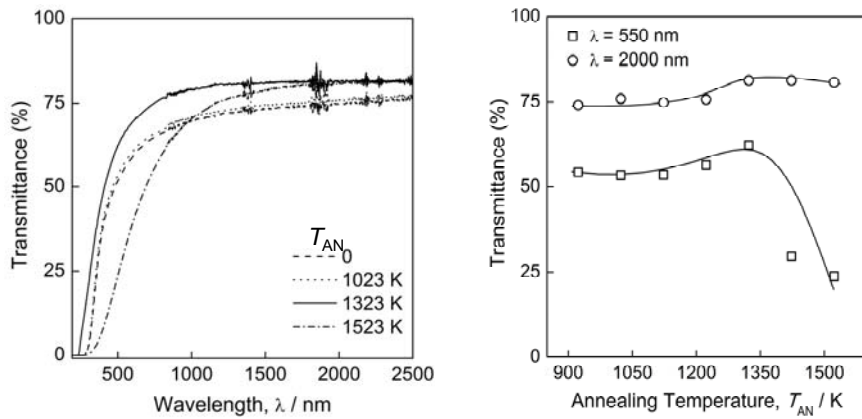
Effect of V_F on Microstructure and Transmittance of Lu_2O_3



- Porosity slightly increased with increasing V_F .
- Transmittance exhibited the maximum at $V_F=0.03 \text{ K s}^{-1}$.

at $P_{pre} = 30 \text{ MPa}$

Effect of annealing on Transmittance of Lu₂O₃



- Annealing can improve the transparency.
- The optimal annealing temperature was 1323 K.

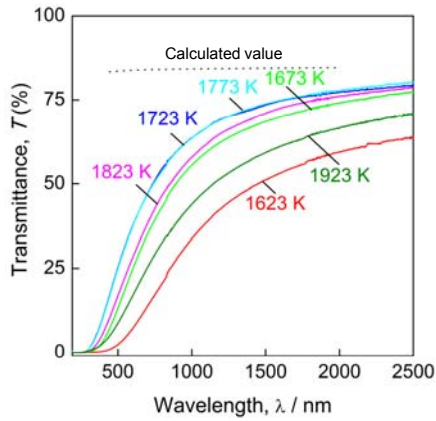
Comparison on Transparency and Grain Size of Lu₂O₃

Sample	Synthesis method	Sintering conditions	Grain size	Transmittance at 550 nm(Thickness)	Reference
5 at.% Eu:Lu ₂ O ₃	VS	1973 K for 5 h	In nano range	Not given (translucent)	E. Zych, J. Alloy. Compd., 34, 391-4 (2002).
0.15 at. % Nd:Lu ₂ O ₃	VS	about 1973 K for 5 h	Not given	Not given (near theoretical value)	J. Lu, Appl. Phys. Lett., 81, 4324-6 (2002).
5 at.% Eu:Lu ₂ O ₃	NPS(H ₂)	2123 K for 6 h	50–60 μm	80% (1 mm)	Q.W. Chen, J. Am. Ceram. Soc., 89, 2038-42 (2006).
3 at.% Nd:Lu ₂ O ₃	NPS(H ₂)	2153 K for 8 h	~50 μm	64% (1.4 mm) 50% for Lu ₂ O ₃	D. Zhou, J. Am. Ceram. Soc., 92, 2182-7 (2009)
5 at.% Eu:Lu ₂ O ₃	VS+ HIP	1873-1923 K for 2h 2123 K, 200 MPa for 4 h	>10 μm	Not given (high) (1.6-1.7 mm)	Z.M. Seeley, Opt. Mater., 33, 1721-6 (2011).
10 at.% Yb:Lu ₂ O ₃	HP +HIP	1873 K for 2h 1873 K, 200 MPa for 2 h	20–50 μm	~80% (3 mm)	J. Sanghera, Opt. mater., 33, 670-4 (2011).
5 at.% Yb:Lu ₂ O ₃	NPS(H ₂)	1953 K for 45 h	Not given	48% (1 mm)	H,J. Zhang, Opt. Mater., in press.
Lu ₂ O ₃	SPS	1723 K, 100 MPa for 2.7 ks	0.91 μm	71.4 % (1 mm)	This work

VS: vacuum sintering, HP: hot pressing, NPS(H₂): pressureless sintering in H₂, HIP: hot isostatic pressing

Nd:Lu₂O₃ by SPS first laser material by SPS

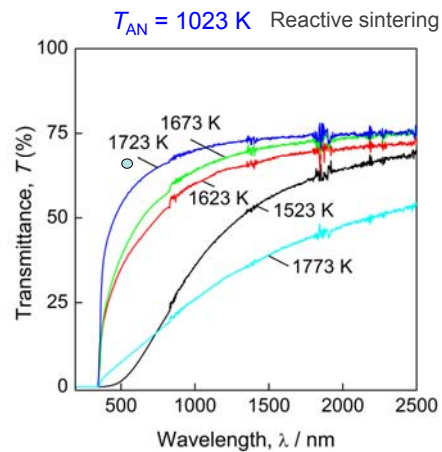
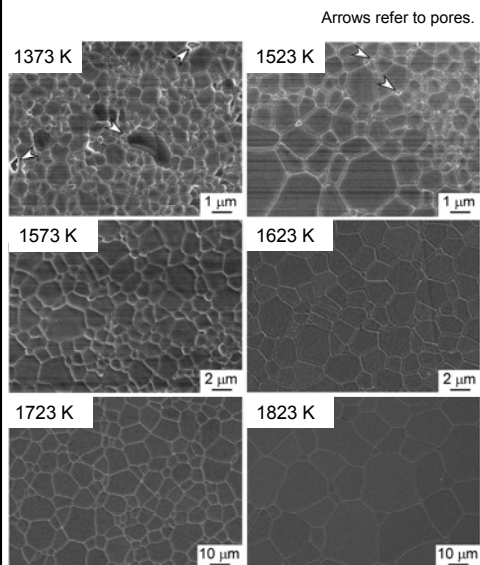
Transmittance of LuAG after Annealing



$$T_{AN} = 1423 \text{ K}$$

- Transparent LuAG was obtained at a relative low sintering temperature of 1723 K.

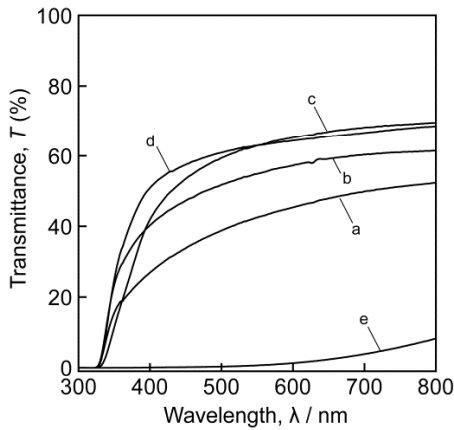
Effect of T_{SPS} on Microstructure and Transmittance of $\text{Lu}_2\text{Ti}_2\text{O}_7$



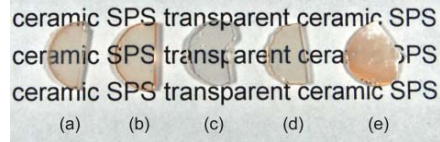
- The calculated value from the refractive index
- The transmittance was 57 and 74% at a wavelength of 550 and 2000 nm, respectively.

Journal of the American Ceramic Society, 94(2011) 3851. An, Ito, Goto

Effect of T_{SPS} on Transmittance of Lu_3NbO_7



Reactive sintering

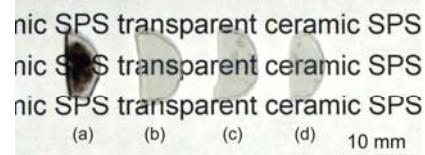
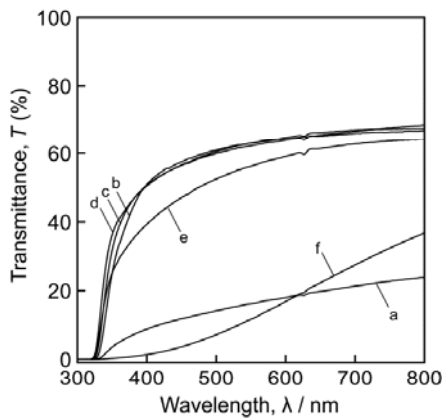


T_{SPS} :
 (a) 1573 K, (b) 1673 K, (c) 1723 K,
 (d) 1773 K, (e) 1823 K

※ Annealed at 1123 K in air for 6 h

- Transmittance increased with increasing T_{SPS} from 1573 (a) to 1773 K (d).
- It became opaque at T_{SPS} 1823 K (e).

Effect of Annealing on Transmittance of Lu_3NbO_7



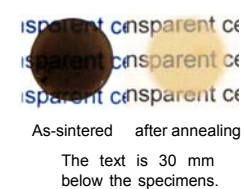
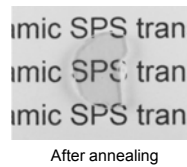
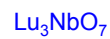
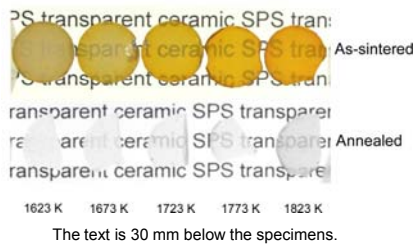
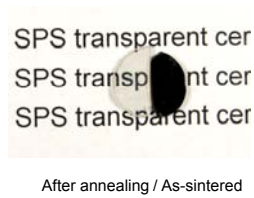
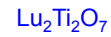
$T_{\text{SPS}} : 1723 \text{ K}$

Annealing at (6h in air):

(a) 1023 K, (b) 1123 K, (c) 1223 K,
 (d) 1323 K, (e) 1423 K, (f) 1523 K

- The rim part became transparent at 1023 K (a).
- The whole part became transparent at 1123-1323 K (b-c).
- It became opaque at 1423 K.

Transparent Lu-based Oxide by SPS



All the specimens are around 10 mm in diameter with 1 mm thickness.

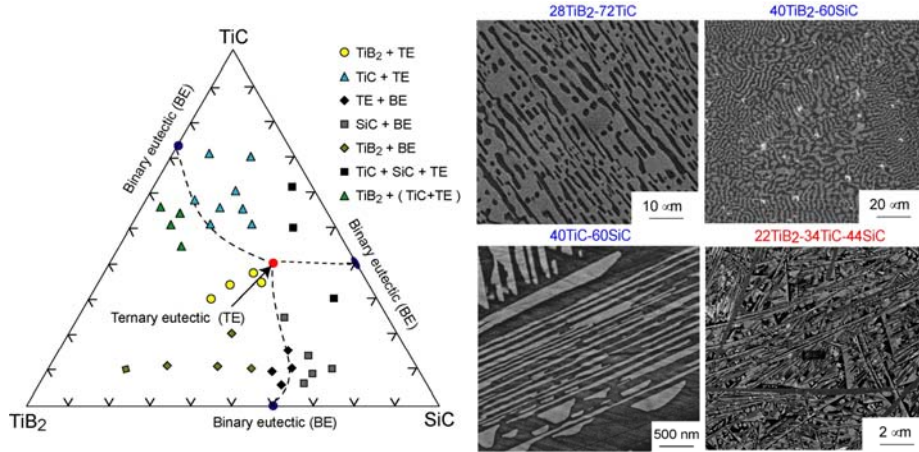
Carbide-Boride Eutectic Composites

- ▣ Carbides: B_4C , TiC , SiC , ZrC , etc.
 - ▣ Borides: TiB_2 , ZrB_2 , etc.
 - ▣ Advantages
 - ◆ High temperature structural materials
 - ◆ Ultrahigh melting point and high hardness
 - ◆ Poor machining performance
- ↓
- Self-assembled composites
- ◆ Eutectic or peritectic reaction
 - ▣ Preparation methods
 - ◆ Floating zone melting
 - ◆ Arc melting

Eutectic composites

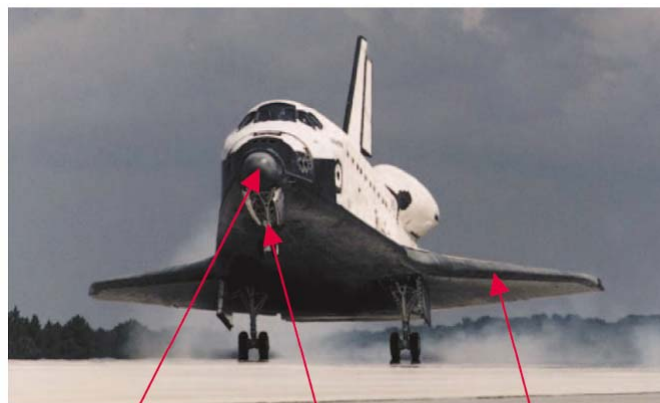
- $\text{B}_4\text{C-TiB}_2$
- $\text{B}_4\text{C-SiC}$
- $\text{B}_4\text{C-TiB}_2\text{-SiC}$
- TiC-TiB_2
- TiC-SiC
- $\text{TiC-TiB}_2\text{-SiC}$
- ZrC-TiB_2
- ZrC-ZrB_2
- SiC-ZrB_2

Phase Diagram of TiC-TiB₂-SiC Ternary System



- Eutectic composites in TiC-TiB₂-SiC system were prepared by arc-melting.

Oxidation Protection System of Shuttle

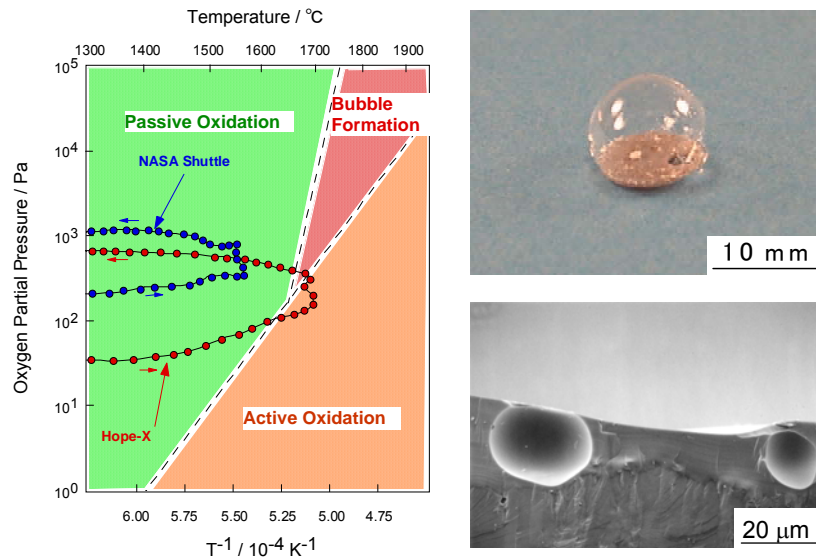


Nose Cap,
Chin Panel,
and Seals

Forward External
Tank Attachment
"Arrowhead" Plate

Wing Leading
Edge Panels
and Seals

Active Oxidation and Bubble Formation at High-Temperature

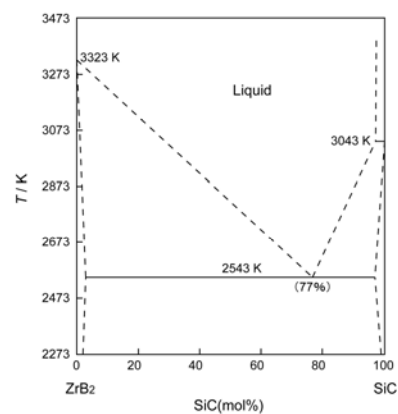


Properties of ZrB₂-SiC Composites

- ZrB₂-SiC is an eutectic system.
- Eutectic composition is not clear.
- Thermal and electrical properties
 - No report
- Mechanical properties

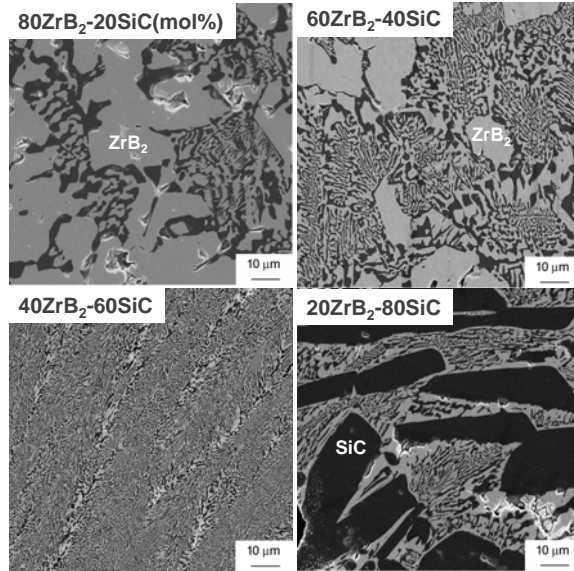
SiC content (vol%)	Modulus (GPa)	Hardness (GPa)	Strength (MPa)	Toughness (MPa m ^{1/2})
0	489	23 ± 0.9	565 ± 53	3.5 ± 0.3
10	450	24 ± 0.9	713 ± 48	4.1 ± 0.3
20	466	24 ± 2.8	1003 ± 94	4.4 ± 0.2
30	484	24 ± 0.7	1089 ± 152	5.3 ± 0.5

Ref: Chamberlain: *J. Am. Ceram. Soc.* 87 (2004) 1170.



Ref: Ordan'yan: *Inorganic Mater.* 25 (1989) 1487.

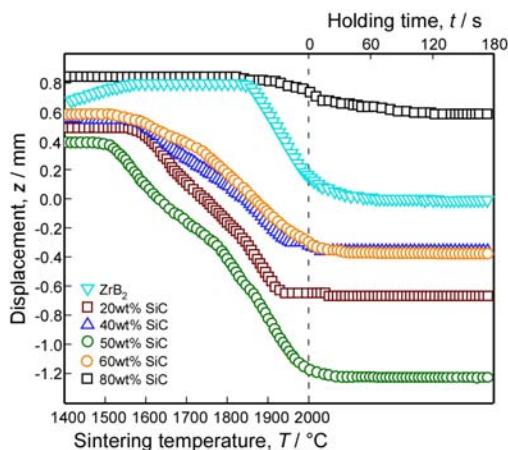
Microstructure of ZrB₂-SiC Composites



- ZrB₂-SiC composites
 - ZrB₂: gray
 - SiC: black
- 40ZrB₂-60SiC(mol%)
 - Uniform microstructure

Sintering of ZrB₂-SiC Composites During SPS

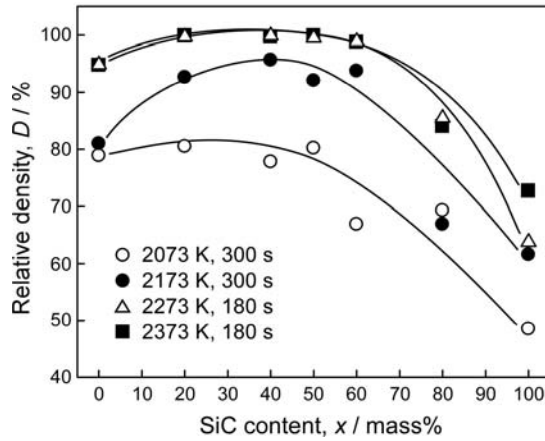
0-80 mass% SiC, 2273 K, 180 s



- Shrinkage completion temperature increased with increasing SiC content.
- Shrinkage of 80 mass% SiC started at 2113 K and displacement continued after holding at 2273 K.
- Shrinkage of composites containing 20-60 mass% SiC completed within 60 s at 2273 K.
- Addition of SiC up to 80 mass% improved densification of ZrB₂.

Relative Density of ZrB₂-SiC Composites

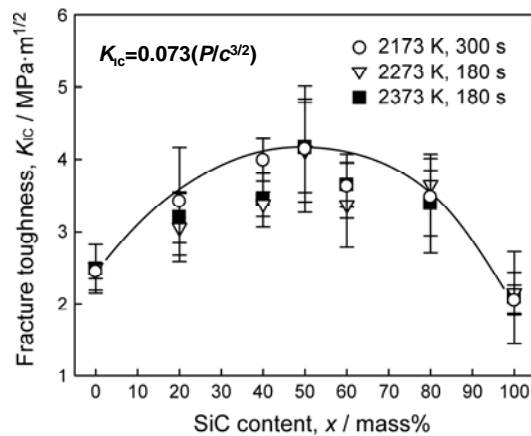
0-100 mass% SiC, 2073-2173 K, 300 s and 2273-2373 K, 180 s



- The addition of 20-60 mass% SiC resulted in increase in relative density at 2173 K.
- 99.9% relative density was obtained for the 20-60 mass% SiC composites at 2273 and 2373 K for 180 s.

Fracture Toughness of ZrB₂-SiC Composites

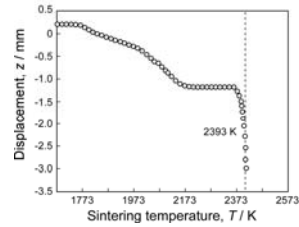
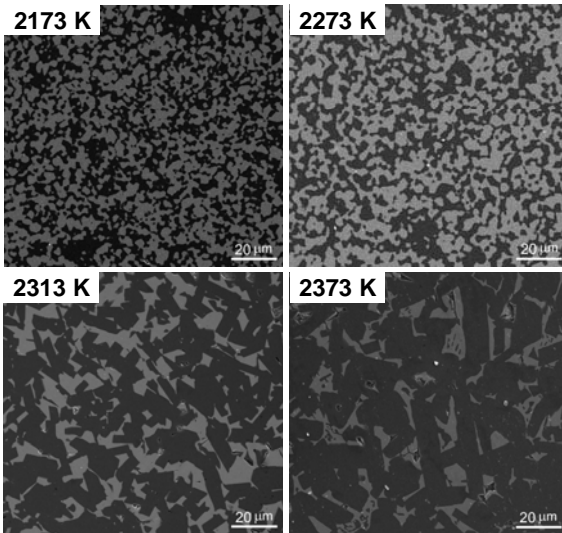
0-100 mass% SiC, 2173 K, 300 s and 2273-2373 K, 180 s



- K_{1c} of ZrB₂-SiC composites decreased with increasing sintering temperature.
- Maximum K_{1c} was obtained for ZrB₂-SiC composites containing 50 mass% SiC for all sintering temperatures.
- When SiC content exceeded 50 mass%, K_{1c} of ZrB₂-SiC composites started to decrease.

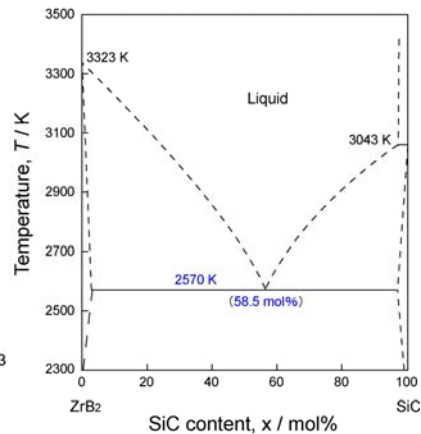
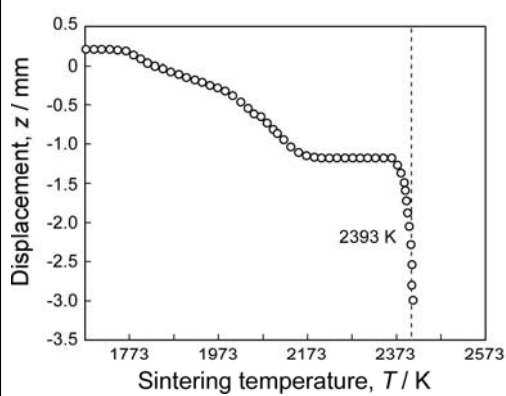
Microstructure of ZrB₂-SiC Composites

40 mass% SiC, 2173 K-300 s, 2373 K-180 s



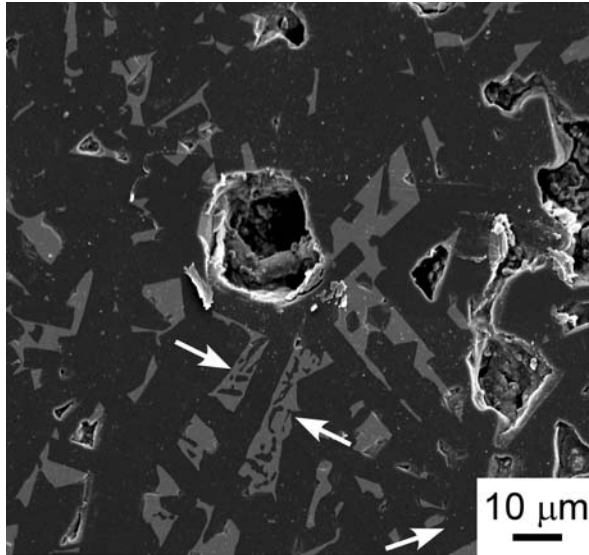
- At 2173 and 2273 K, microstructures comprise equiaxed ZrB₂ and α-SiC grains.
- Elongated α-SiC grains formed at 2313 K and irregular texture composed of ZrB₂ and fine α-SiC grains were observed at 2373 K.

Melting Point of ZrB₂-SiC Eutectic Composites



- Spark plasma sintering
 - ◆ Heating to be melted
- Melting point: 2570 K
- Eutectic composition:
 - ◆ 41.5ZrB₂-58.5SiC (mol%)
- Eutectic melting point:
 - ◆ 2570 K

Local Structure of ZrB₂-SiC Eutectic Composites



Eutectic Temperature
2570 K

Sintering Temperature
2373 K

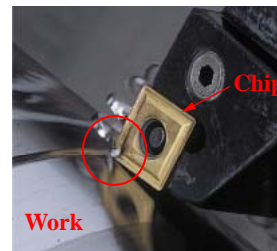
Cutting Tools



Chip



Drill



Harsh environment at the chip edge



Milling cutter



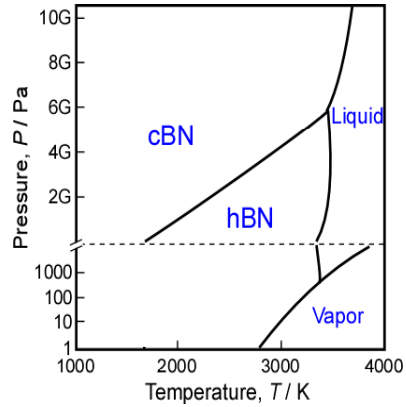
Endmill



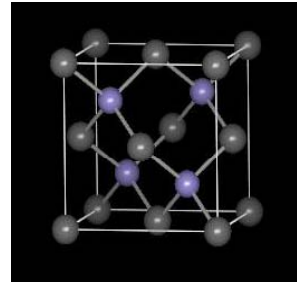
Requirements

- ▶ High hardness
- ▶ High toughness
- ▶ High thermal stability

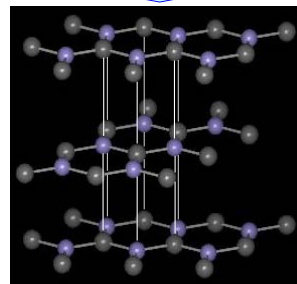
Cubic Boron Nitride (cBN)



cBN



hBN



- ▶ Non-sinterability
- ▶ Transformation to hBN at high temperature

Fabrication of cBN Cutting Tools

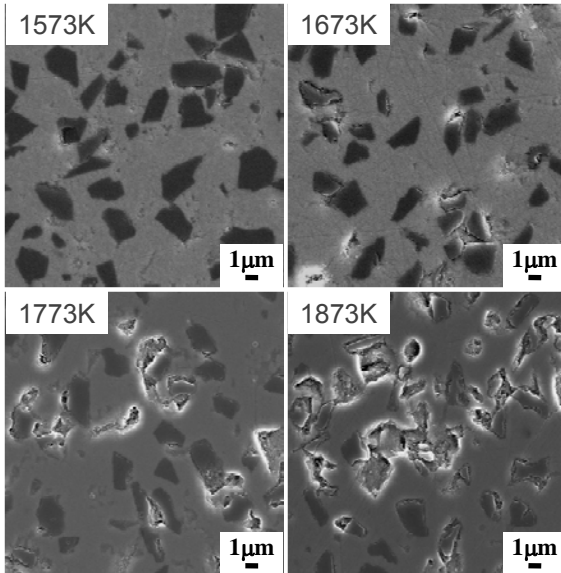
Ultra-high pressure (>5GPa) sintering of cBN or hBN with binders such as metal Al and TiC



Moderate pressure (<100 MPa) hot- pressing
More practical applications

Microstructure of Al₂O₃-cBN Composite

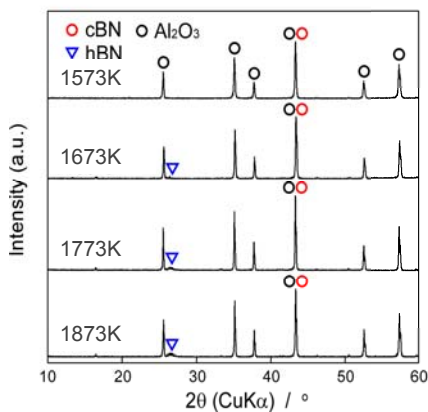
20vol%cBN, 1573-1873K, 600s



- Sharp edged well adhered cBN particles at 1573K
- A small amount of voids and cracks around cBN particles at 1673K
- Phase transformation of cBN to hBN at 1773-1873K

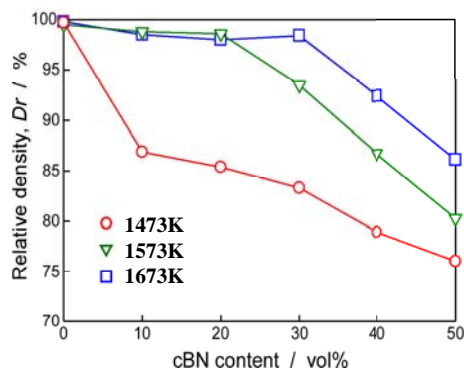
XRD Profiles of Al₂O₃-cBN Composites

20vol%cBN, 1573-1873K, 600s



- A slight transformation to hBN at 1673K.

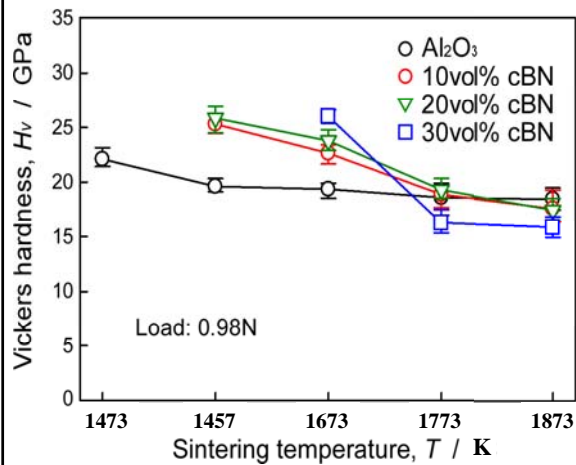
0-50vol%cBN, 1473-1673K, 600s



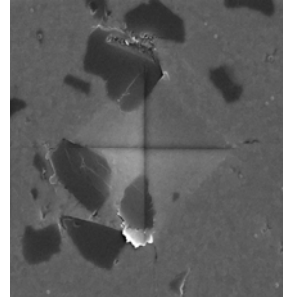
- Density of more than 98% at 1573-1673K (10-20vol%cBN)

Vickers Hardness of Al₂O₃-cBN Composite

0-30vol%cBN, 1473-1873K, 600s



20vol%cBN, 1573K



$H_v = 26 \text{ GPa}$

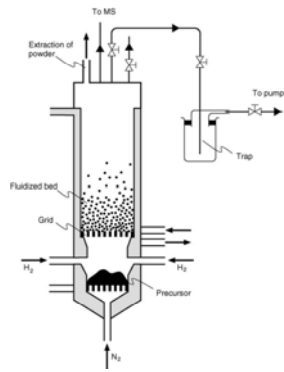
■ The highest hardness of 26GPa at 1573K (20vol% cBN)

Strategy to Consolidate cBN Powder

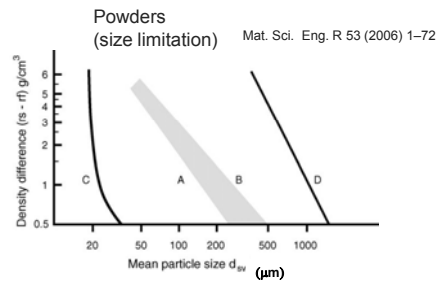
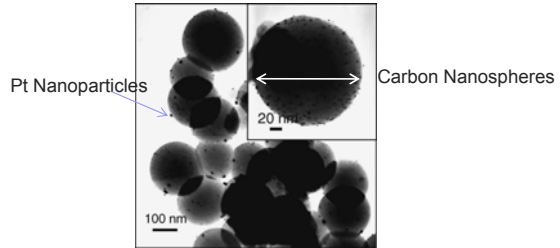
- Modification of Powder Surface (Coating)
 - ◆ Fluidized bed CVD (FBCVD)
- Rotary CVD
- Nano-particle/Nano-film Coating on Powders
 - ◆ Ni, SiO₂ Coating on cBN Powder
- Consolidation of cBN-base Composites by SPS

CVD Coating of Particle/Film on Powder

Fluidized bed CVD



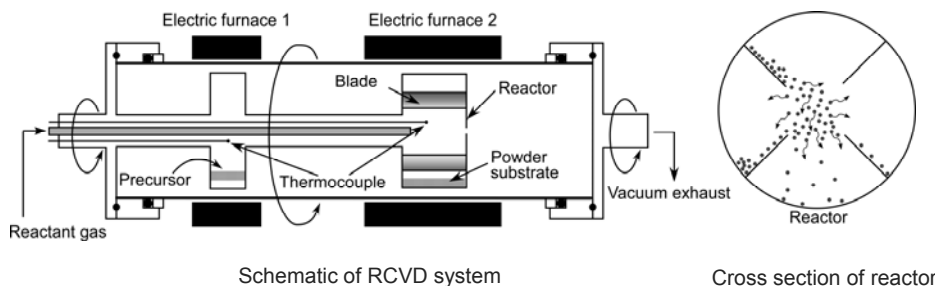
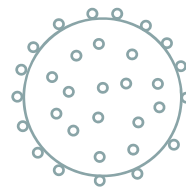
Most frequently employed CVD technique for deposits on powders



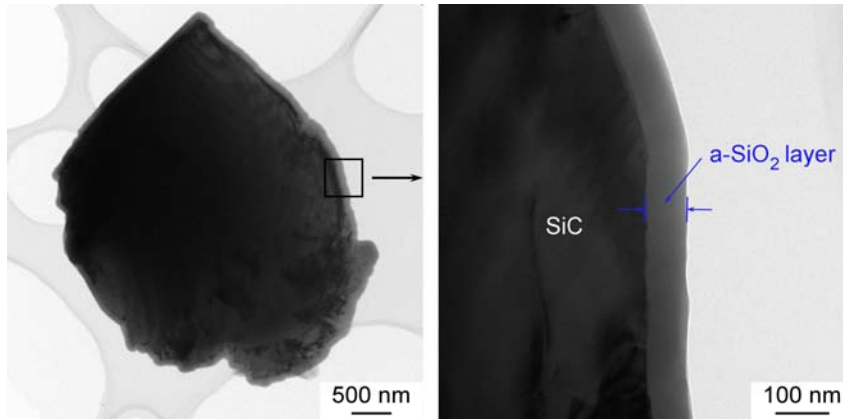
Difference between the density of the powder and that of the fluidizing gas

Surface Modification of cBN Powder by Rotary CVD

Surface modification of powder
Nano-particle on powder
↓
Accelerate sintering (SPS)
↓
High performance materials
New functional materials

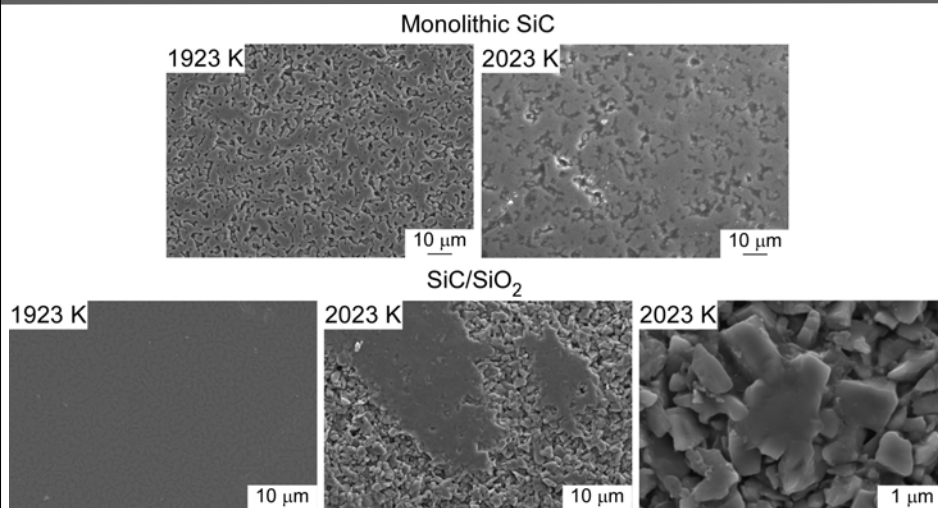


Morphology of SiO₂-coated SiC Powder



- Amorphous SiO₂ was uniformly coated on SiC particles, and the nano-layer thickness of the a-SiO₂ ranged from 60 to 80 nm at deposition time of 7.2 ks.
- The SiO₂ mass content in the SiC/SiO₂ powder was estimated at 22 mass% by mass gain after RCVD.

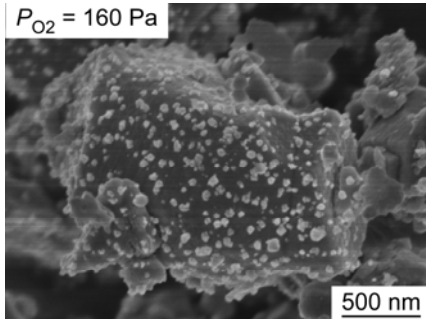
Polished surface morphology of sintered body



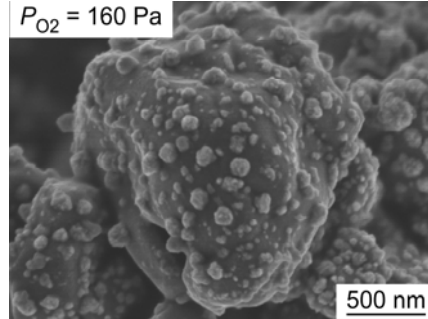
- Compared with monolithic SiC, SiO₂ prevented the grain growth of SiC.
- At 2023 K, SiO₂ reacted with SiC, and Si was produced.

SEM images of Ni Precipitated TiC, TiCN Powder

Ni precipitated TiC powder



Ni precipitated TiCN powder



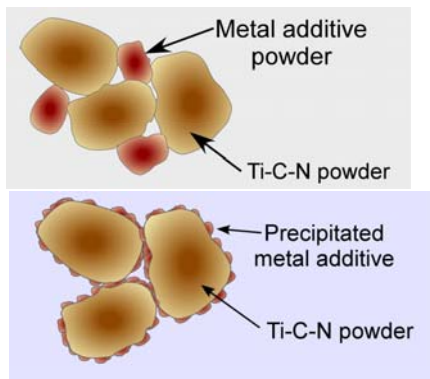
Precipitated phase

- $P_{O_2} = 0$ Pa: single phase Ni
- $P_{O_2} = 80\sim 160$ Pa: Ni + NiO
- $P_{O_2} = 240$ Pa: NiO + TiO₂

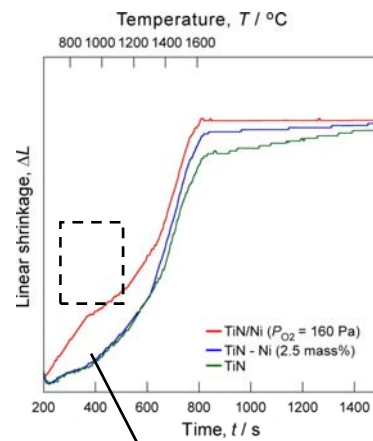
Microstructure

- Ni or NiO nanoparticle about 20~100 nm in diameter was precipitated.
- ➡ Ni nanoparticles were uniformly precipitated.

Sintering Behavior of Ni Nano-Particle Precipitated TiCN

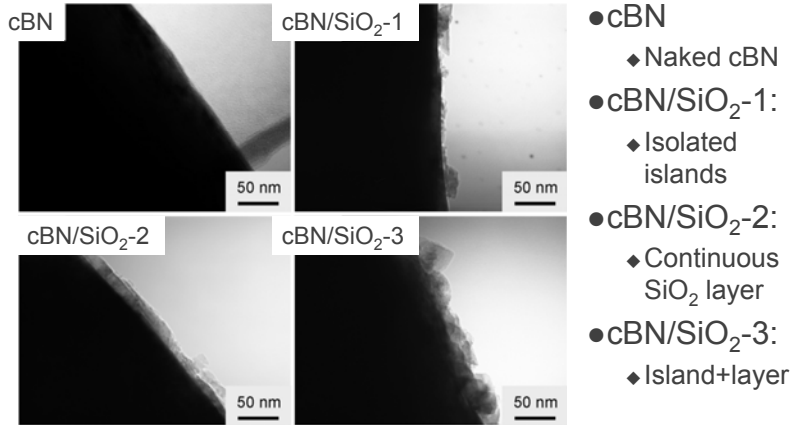


- Shrinkage at a low temperature region



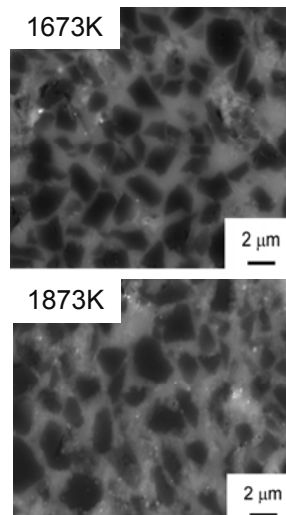
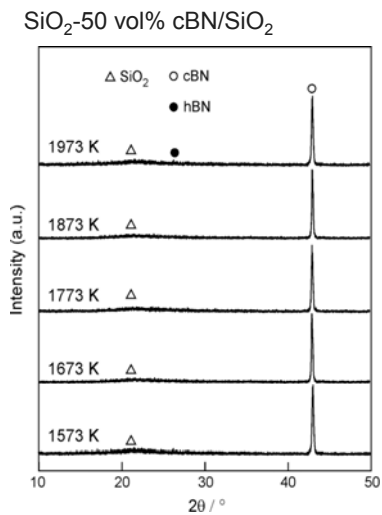
0.56~0.68 $T_m(\text{Ni})$

TEM Images of cBN/SiO₂ Powder



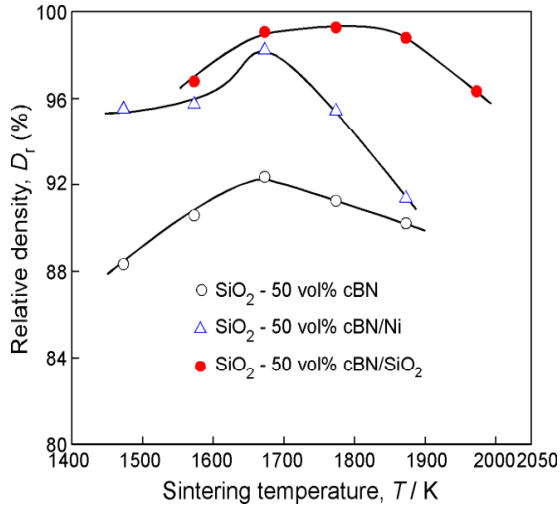
$$R_s: \begin{array}{l} 1: 5.56 \times 10^{-9} \text{ m}^3 \text{ s}^{-1} \\ 2: 11.11 \times 10^{-9} \text{ m}^3 \text{ s}^{-1} \\ 3: 16.67 \times 10^{-9} \text{ m}^3 \text{ s}^{-1} \end{array}$$

XRD Patterns of SiO₂-cBN Composites



- 50 vol% cBN/SiO₂ composites
 - ◆ Phase transformation of cBN to hBN occurred at 1973 K.

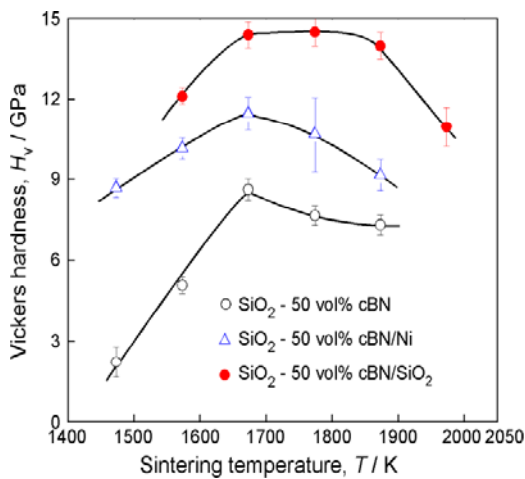
DENSITY OF SiO₂-cBN COMPOSITES



- SiO₂-(40-50) vol% cBN/SiO₂ composites was almost fully densified.

Ni content in cBN: 1.6 mass%

HARDNESS OF VARIOUS SiO₂-cBN COMPOSITES



- Hardness increased by coating Ni and SiO₂ on cBN powder.

- The highest hardness was 14.5 GPa (50 vol% cBN/SiO₂).

Ni content in cBN: 1.6 mass%

Summary

- SPS (Spark Plasma Sintering)
Spark? Plasma? Unknown
- ECAS (Electric Current Activated/Assisted Sintering)
Mass Transport by Electric Field? Unknown
- ▣ Effects of SPS
Non-Sinterable Refractory Material, Easy-to-decompose Materials
in a short time (within a few minutes)
Meta-stable or Non-stable Materials are sinterable.
 - ✓ Excess surface energy (Stress on the surface, Defects...)
 - ✓ Re-arrangement and desiccation before neck growth
- ▣ Future Study
 - ✓ Sintering Mechanism
 - ✓ Non-sinterable Material → Surface Modification of Powder